

Relative stability of zincblende and wurtzite structure in CdX(X = S, Se, Te) series - A NMTO study

Soumendu Datta¹, Tanusri Saha-Dasgupta^{1†} and D. D. Sarma^{2,3}

¹S.N. Bose National Centre for Basic Sciences, Kolkata 700 098, India

² Centre for Advanced Materials, Indian Association for the Cultivation of Science, Jadavpur, Kolkata 700 032, India

³ Solid State and Structural Chemistry Unit, Indian Institute of Science, Bangalore 560 012, India

1. Introduction

Tetrahedrally coordinated binary semiconductors of $A^N B^{8-N}$ type having total of 8 valence electrons are compounds of great technological importances. They have been widely studied both theoretically and experimentally[1, 2]. An interesting aspect of these compounds is that they can belong to either cubic or in hexagonal symmetry, namely in zincblende(ZB) or in wurtzite(WZ) structure. The difference between the two structures is subtle, both being of tetrahedral coordination, and also the associated total energy difference is small, of the order of few tens of meV/atom. These particular aspects have made the ZB vs WZ structural stability issue a topic of significant interest that have been discussed in literature both in terms of model calculations as well as in terms of first principle calculations[3, 4, 5, 6, 7, 8, 9, 10, 11, 12]. Phillips and Van Vechten [5] first gave a well defined prescription in terms of ionicity to predict the crystalline phase in binary octet semiconductors of $A^N B^{8-N}$ type, with the help of the dielectric theory. While their theory nicely described the transition from four-fold to six-fold coordination and possibly also to eight-fold coordination, it was not able to distinguish clearly between structures having the same coordination. P. Lawaetz[7] investigated the stability of WZ structure more closely. Taking into account the short-range elastic forces and long-range Coulomb forces, he correlated the ZB vs WZ stability with the deviation of the axial ratio $\frac{c}{a}$ from the ideal value, which was further related with a structure-independent charge parameter. However, the results were not fully satisfactory because of limited knowledge about the long-range Coulomb-effects in partially ionic materials. Christensen et al. [11] studied the structural phase stability

† email : tanusri@bose.res.in

of 34 elemental and compound semiconductors from first principle electronic structure calculations which involved mostly four-fold to six-fold coordination transitions. They studied the chemical trends by calculating the valence charge densities using linearized muffin-tin orbital (LMTO) based localized basis sets. Their calculated ionicities from tight-binding representation of LMTO Hamiltonian, gives better chemical trend than Phillips value. Recently, the ZB - WZ polytypism in binary octet semiconductors have been studied by the group of Alex Zunger[12] in terms of quantum mechanically defined atomic-orbital radii. They showed a linear scaling between the ZB - WZ energy difference and renormalized orbital radii and successfully predicted the exact structural trends in most of the octet compounds, except some few cases. The general understanding that emerged out of these calculations is that it is the competition between the covalency and the ionicity effects that determines the relative stability of ZB vs WZ structures, with covalency favoring ZB structure and ionicity favoring wurtzite structure.

Experimentally, the stable crystal phase of CdS is hexagonal wurtzite structure[13]. For CdSe, zincblende is the stable low temperature phase and above a critical temperature, it transforms to wurtzite structure[14]. On the other hand, CdTe always stabilizes in cubic zincblende structure[15]. However, there is a few indication of metastable wurtzite growth for CdTe in some special situation[16]. In the present work, we revised the issue of relative stability of ZB and WZ in the CdX series, with $X = S, Se, Te$ using Nth-order muffin-tin orbital (NMTO) technique[17] within the framework of density functional theory (DFT). In particular, we employed the “direct generation of Wannier-like orbitals” feature of NMTO technique for attaining the microscopic understanding in this context.

2. Crystal structure

The ZB structure consists of two interpenetrating face centered cubic(FCC) sublattices, one of atom A, the other of atom B, displaced from each other along the body diagonal by $\frac{a}{4}$, a being the lattice constant for the ZB structure. On the other hand, an ideal WZ structure consists of two interpenetrating hexagonal closed packed(HCP) sublattices, one of atom A, the other of atom B, displaced from each other by $\frac{3}{8}c$ along the c -axis. These result into two different stacking sequences: ABCABC... along [111] direction for ZB and ABAB... along c -axis for WZ. The ZB structure corresponds to the *staggered* conformation of atomic arrangement along [111] body diagonal, while the wurtzite structure corresponds to the *eclipsed* conformation as seen looking down the c -axis. The nearest neighbor (tetrahedral bond) arrangements in the ZB structure and in the ideal WZ structure are identical. The main difference starts to come in the relative position of 3rd nearest neighbors and beyond. Also the arrangement of the distant atoms along the four different tetrahedral bonds are different for a WZ structure. The structural differences between these two phases have been shown in Fig. 1.

The lower symmetry of the WZ structure allows for a distortion with the c/a ratio

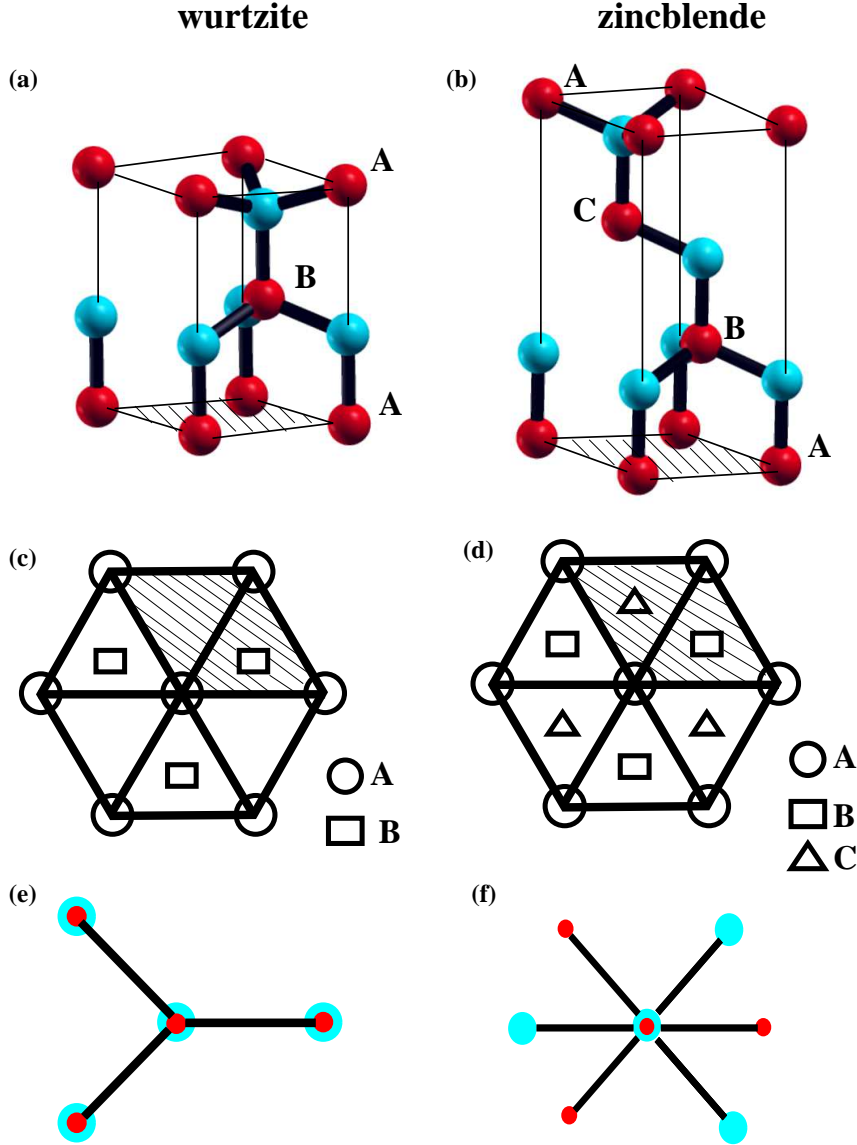


Figure 1. (a) and (b) show the crystal structure in WZ and ZB symmetries. Two different colored atoms denote cation and anion. (c) WZ structure shows the ABAB... stacking of atoms, while (d) ZB structure shows the ABCABC... stacking. *Eclipsed* and *staggered* conformation of atoms along c -axis in WZ structure and along $[111]$ body diagonal in ZB structure have been shown in (e) and (f) respectively.

deviating from the ideal value of $\sqrt{\frac{8}{3}} = 1.633$. A further kind of distortion, that is possible in the hexagonal structure and forbidden in the cubic, is that the two interpenetrating sublattices are slightly displaced from each other so that an atom of one sublattice is no longer at the centroid of the other sublattice. In order to capture these distortions, it is necessary to define another internal parameter “ u ”, which is the nearest neighbor distance along c -axis, in unit of c . The value u in the ideal WZ structure is $\frac{3}{8} = 0.375$. Distortion of u from its ideal value gives rise to a dipole at the center of each tetrahedron, containing an atom of opposite kind, the magnitude of which depends

upon Δu [$\Delta u = u - 0.375$] and the ionicity of the chemical bonds. This effect also lowers the ionization energy. The structural parameters of CdS, CdSe and CdTe used in the present calculation are listed in Table 1.

Table 1. Structural parameters of ZB and WZ phases for CdX (X = S, Se, Te) series. Lattice parameters have been taken from Ref. [12] for both ZB and WZ phases of CdS, from Ref. [18] for ZB CdSe, from Ref. [19] for WZ phase of CdSe, from Ref. [15] for ZB CdTe and from Ref. [16] for WZ CdTe.

Compounds	WZ					ZB
	$a(\text{\AA})$	$\frac{c}{a}$	u	$\Delta(\frac{c}{a})$	Δu	$a(\text{\AA})$
CdS	4.121	1.621	0.377	-0.012	0.002	5.811
CdSe	4.299	1.631	0.376	-0.002	0.001	6.077
CdTe	4.57	1.637	0.375	0.004	0.000	6.492

It shows that the deviation $\Delta(\frac{c}{a})$ [$\Delta(\frac{c}{a}) = \frac{c}{a} - 1.633$] is -ve and largest for CdS, while it is +ve for CdTe. The deviation from the ideal c/a ratio is tiny for CdSe. The deviation Δu is found to be opposite in sign to that of $\Delta(\frac{c}{a})$. A part of the deviation Δu is expected to come due to nearest neighbor bond bending or bond stretching caused by $\Delta(\frac{c}{a})$. The limits on this part, as calculated by Keffer and Portis[4] for AlN, are $u = 0.380$ to maintain equal nearest neighbour bond lengths and $u = 0.372$ to maintain equal four tetrahedral angles. However, measured value of u for AlN is 0.385[4]. This means there must be additional contribution in the distortion of u from ideal value, which is coming from the long-range Coulomb interaction. NMTO technique based on full self-consistent DFT calculations includes both the effect of short-range as well as long-range interaction in providing a complete understanding.

3. Total energy calculations

In order to check the relative stability of the ZB and WZ structures of the CdS, CdSe and CdTe, we carried out total energy calculations using the energetically accurate pseudo-potential basis set. The calculations have been performed with ultra-soft pseudopotential[20] and local density approximation for the exchange-correlation functionals implemented in the Vienna *Ab-initio* Simulation Package(VASP)[21]. The wavefunctions are expanded in the plane wave basis set with a kinetic energy cut-off of 250 eV which gives convergence of total energy sufficient to discuss the relative stability of various phases. The calculations have been carried out with a k-space grid of $11 \times 11 \times 11$. The obtained total energies and the band gaps are listed in Table 2. As found, the total energy differences are indeed very tiny; of the order of few meV. Our calculations correctly show that CdS to be stable in WZ phase and CdTe to be stable in ZB phase. CdSe which is considered as a boarder line case is found to be

stable in ZB phase in agreement with the published results[12]. The band gaps in WZ and ZB structures, both being direct band gaps for CdS, CdSe and CdTe are similar for a given compound. It is found that the band gap decreases monotonically in moving from CdS to CdTe in both ZB and WZ symmetries. This monotonic decrease in band gap indicates the enhanced metallicity across the CdS-CdSe-CdTe series which points to CdTe being more covalent compared to CdS.

Table 2. Total energy per formula, energy difference $\Delta E = E(ZB) - E(WZ)$ and band gaps. + ve sign of ΔE indicates WZ is more stable than ZB and vice versa. The numbers within the parenthesis in the columns of band gap, correspond to their experimental values taken from Ref. [22]

Compounds	Energy(eV/formula)		ΔE (meV)	Band gap(eV)	
	ZB	WZ		ZB	WZ
CdS	-6.8650	-6.8665	1.5	0.94(2.55)	1.02(2.58)
CdSe	-6.7548	-6.7523	-2.5	0.77(1.90)	0.72(1.83)
CdTe	-6.0248	-6.0221	-2.7	0.69(1.60)	0.65(1.60)

4. Calculation of ionicity

As already pointed out, the relative stability between ZB and WZ phases of $A^N B^{8-N}$ semiconductors is dictated by the competition between the covalent bonding and the electrostatic energy given by the difference between the cation and anion energy levels. In a homopolar semiconductors like Si, it is only the first term that survives. For a tetrahedrally coordinated semiconductor, it is most natural to think in terms of sp^3 hybrids. Considering the sp^3 hybrid energy as $E_{sp^3} = \frac{E_s + 3E_p}{4}$ the energy level separation between cation and anion is given by $\Delta E_{sp^3} = E_{sp^3}^c - E_{sp^3}^a$; where c and a denote cation and anion respectively. The hybridization contribution on the other hand is related to the hopping integral between the cation and anion sp^3 hybrids. It is given by $h = \frac{1}{4} \langle s^a + p_x^a + p_y^a + p_z^a | H | s^c - p_x^c - p_y^c - p_z^c \rangle$ considering the [111] bond of ZB structure and $h = \frac{1}{2} \langle s^a + p_z^a | H | s^c - p_z^c \rangle$ considering the [001] bond of WZ structure where H is the tight binding Hamiltonian in the sp basis of cation and anion. The ionicity is then defined as

$$f_i = \frac{(\Delta E_{sp^3})^2}{(\Delta E_{sp^3})^2 + (2h)^2} \quad (1)$$

In order to extract the energy level separation and the hopping interaction, we employed the NMTO-downfolding technique. In this method, a basis set of localized orbitals is constructed from the exact scattering solutions (partial waves and Hankel functions) for a superposition of short-ranged spherically-symmetric potential wells, a so called

muffin-tin (MT) approximation to the potential. The basis set is constructed from the scattering solutions at a mesh of energies, $\epsilon_0, \epsilon_1, \dots, \epsilon_N$. At those energies, the set provides the exact solutions, while at other energies, E , the error is proportional to $(E - \epsilon_0)(E - \epsilon_1) \dots (E - \epsilon_N)$. The basis set of NMTOs is therefore selective in energy. Moreover, each NMTO satisfies a specific boundary condition which gives it a specific orbital character and makes it localized. The NMTO basis set due to its energy selective character is flexible and can be chosen as minimal via the downfolding procedure which integrates out the degrees of freedom that are not of interest. The downfolded NMTO set spans only the selected set of bands with as few basis functions as there are bands. For the isolated set of selected bands the NMTO set spans the Hilbert space of the Wannier functions, that is, the orthonormalized NMTOs are the Wannier functions. The Wannier orbitals are therefore generated directly in this method, which may be contrasted with the techniques where Wannier functions are generated out of the calculated Bloch functions as a post processing step[23]. The downfolded Hamiltonian in the Wannier basis provides the estimates of onsite energies and the hopping integrals.

In order to compute the ionicity parameter defined in Eqn. (1), the NMTO calculations have been carried out with Cd(*spd*) and X(*sp*) basis. NMTO calculations being not yet implemented in self-consistent form, the self consistent calculations have been carried out in the LMTO method. The self consistent MT potential out of these LMTO calculations has been used for the constructions of NMTOs, which in the present case is the standard LMTO all-electron CdXEE' atomic spheres potential for the ZB structure and Cd₂X₂E₂E'₂ for the WZ structure. E and E' are two different empty spheres used to fill the space. The calculated estimates of ΔE_{sp^3} , hopping integral h and ionicity parameter f_i for CdX series are listed in Table 3. The NMTO approach successfully brings out the right trend within the CdX series both for the ZB and the WZ structures, i.e CdS has the maximum ionicity and CdTe has the least. For comparison, the results of previous calculations by Christensen et al.[11] using the tight-binding LMTO approach and that by Phillips [2] using dielectric theory are also listed. As it is found, while NMTO could bring out the right trend within the fine differences, the two previous approaches could not capture it properly.

Table 3. Covalent gap ΔE_{sp^3} , hopping term $E_h = -2h$ and ionicity f_i for the CdX series in ZB and WZ structure. $f_i(C)$ means calculated value of ionicity by Christensen et al. [11] and $f_i(P)$ that of Phillips taken from Ref.[2]

Compounds	ΔE_{sp^3} (eV)		$E_h = -2h$ (eV)		f_i		$f_i(C)$		$f_i(P)$	
	ZB	WZ	ZB	WZ	ZB	WZ	ZB	WZ	ZB	WZ
CdS	7.13	7.17	6.37	6.29	0.556	0.565	0.794	...	0.685	...
CdSe	6.70	6.69	6.16	6.04	0.542	0.551	0.841	...	0.699	...
CdTe	5.36	5.45	5.79	5.74	0.462	0.475	0.739	...	0.717	...

5. Microscopic understanding in terms of calculated Wannier functions

In order to gain further insights, we went a step ahead and constructed the truly minimal NMTO sets with the sp -orbitals placed exclusively on the anion(X) site and downfolded all the orbitals at the cation(Cd) site, except the cation d orbitals. This gives rise to the basis with only 4 sp -orbitals out of 8 sp -orbitals in the ZB unit cell and 8 sp -orbitals out of 16 sp -orbitals in the WZ unit cell. The energy points are chosen in the way so as to span only the valence bands. The comparison of the downfolded valence-only bands and the full band structure can be made as good as possible by making the energy mesh finer and finer. The plot shown in Fig.2 for CdS with the choice of 4 energy points already shows the downfolded bands to be indistinguishable from the full band structure in the scale of the plot. Similar agreements are found also for CdSe and CdTe .

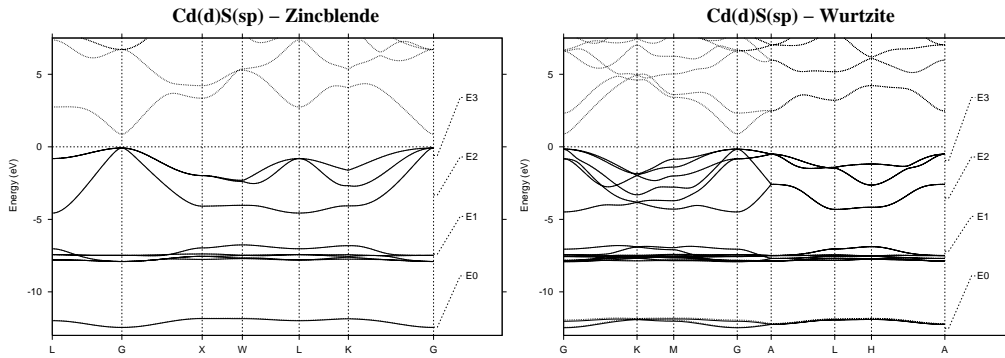


Figure 2. Downfolded bands (thick line) with the basis sets where sp -MTOs are on S atom and d -MTOs are on Cd atom, are compared with NMTO all bands (thin line) both in ZB(left) and WZ(right) structure of CdS . The energy mesh for downfolding have also been shown.

Fig.3 shows the plot of the orthonormalized p -NMTO ($N=3$) centered at the anion site and pointing to the neighboring Cd site along the $[111]$ direction for the ZB structure and $[001]$ direction for the WZ structure. As it is clearly seen, the red lobe at the left-hand side which is a mark of the covalency effect, systematically increases in moving from S to Se to Te. Had it been plotted for the case of homopolar system like Si which is a perfectly covalent compound, the plot would have been perfectly symmetric with the red lobes being symmetric between left hand and the right hand side. These plots reconfirm the conclusion that the ionicity decreases and the covalency increases across the CdX series.

Fig. 4 shows the plots of directed p -NMTO same as in Fig. 3 but for four different tetrahedral bond directions of WZ and ZB structure for CdS . While the four bond-centered p -NMTOs look identical for ZB structure, the bond-centered p -NMTO directed along the $[001]$ direction of the WZ structure, looks different from the rest of the three. The difference primarily comes from the tail sitting at Cd position at $c(1-u)$ measured from the central anion position at $X(0,0,0)$ along the $[001]$ axis (see Fig. 5). There is no equivalent neighboring atom along three other directions.

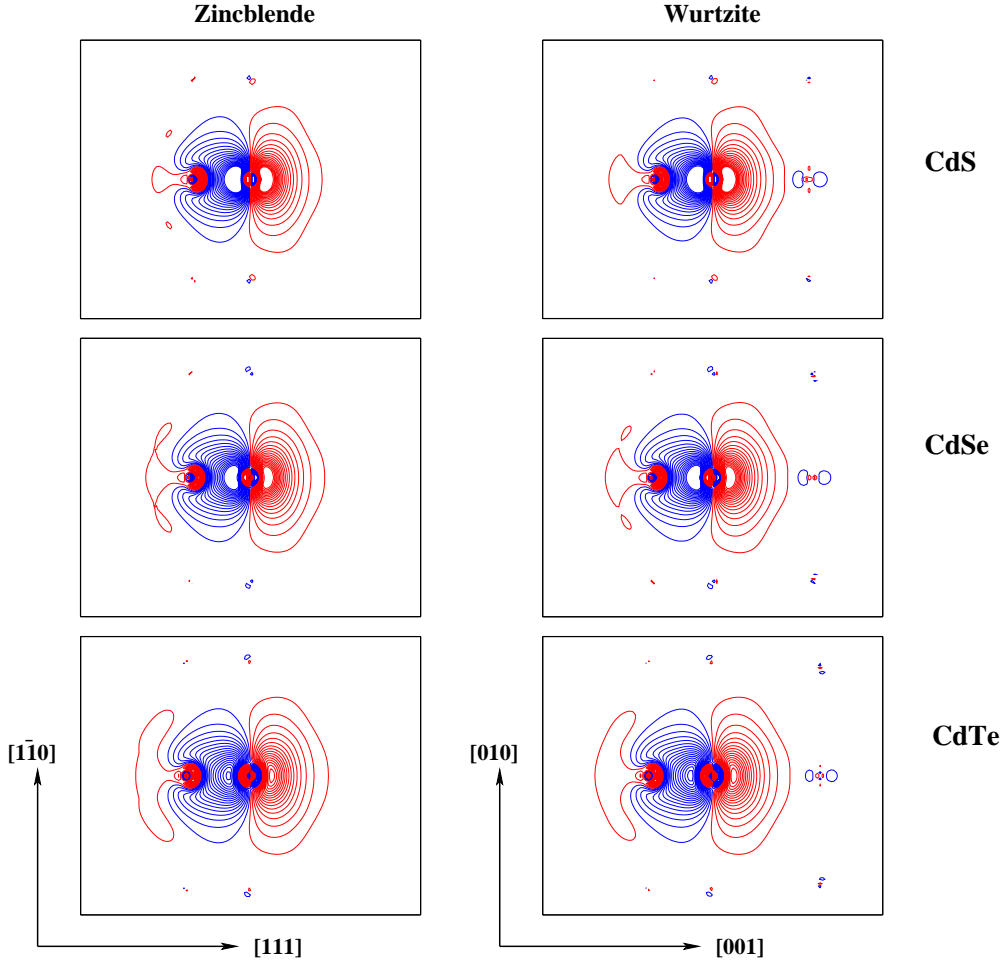


Figure 3. The contour plots show the anion $p[111]$ MTO in ZB structure (left panels) and anion $p[001]$ MTO in WZ structure (right panels) of CdX ($X = \text{S}, \text{Se}, \text{Te}$). The top most panels correspond to CdS and the bottom most to CdTe. In each case, 35 contours have been drawn in the range -0.15 to 0.15 electrons/Bohr³. From top to bottom, the ionicity decreases and the covalency increases.

In order to understand this effect, we have carried out model calculations where $\Delta\left(\frac{c}{a}\right)$ ratios have been made -0.1, -0.05 and 0.1. The corresponding “u” parameter in each case has been obtained by total energy minimization fixing the lattice parameters. The deviation in “u”, Δu is found to roughly obey the relationship with $\Delta\left(\frac{c}{a}\right)$ as $\Delta u = -\left(\frac{3}{128}\right)^{\frac{1}{2}} \xi \Delta\left(\frac{c}{a}\right)$ where ξ , the bond-bending parameter, is 2.0, given by P. Lawaetz[7]. We computed the ionicity parameter f_i for each of the model systems by NMTO downfolding technique. In Table 4 we list the ionicity parameter for the model WZ systems, together with actual CdTe case. As it is evident the -ve deviation from ideal $\left(\frac{c}{a}\right)$ ratio makes the compound more ionic as pointed out previously. Changing $\Delta\left(\frac{c}{a}\right)$ ratio from -ve to +ve passing through the ideal $\Delta\left(\frac{c}{a}\right)$ ratio, the ionicity decreases and covalency increases. This is in agreement with the structural parameters of CdS, CdSe and CdTe. CdS being

the most ionic among the three, shows the largest negative deviation in $\left(\frac{c}{a}\right) \cdot \left(\frac{c}{a}\right)$ ratio for CdSe is close to ideal, while deviation in $\left(\frac{c}{a}\right)$ ratio for CdTe becomes positive.

Table 4. Covalent gap ΔE_{sp^3} , hopping term $E_h = -2h$ and ionicity f_i for model CdTe in WZ structure, with $\Delta\left(\frac{c}{a}\right)$ and u as given in the first column.

CdTe	ΔE_{sp^3} (eV)	$E_h = -2h$ (eV)	f_i
$\Delta\left(\frac{c}{a}\right) = -0.100$ and $u = 0.4044$	5.49	5.33	0.515
$\Delta\left(\frac{c}{a}\right) = -0.050$ and $u = 0.3903$	5.48	5.57	0.491
$\Delta\left(\frac{c}{a}\right) = +0.004$ and $u = 0.375$	5.45	5.73	0.475
$\Delta\left(\frac{c}{a}\right) = +0.100$ and $u = 0.3432$	5.45	6.13	0.441

In Fig. 6, we show the downfolded p-NMTO for the model WZ systems together with actual WZ CdTe system along [001] direction and one of the three other directions, namely $[-1, 0, \frac{u}{\sqrt{3}}\frac{c}{a}]$. As it is evident, changing $\Delta\left(\frac{c}{a}\right)$ from -ve to +ve makes the two p-NMTOs directed along the vertical [001] bond and one of the other directions, looking alike, diminishing the tail effect sitting at Cd[0, 0, c(1 - u)] site. This is driven by the covalency effect which prefers an isotropic arrangement. However, it cannot be completely achieved within a hexagonal symmetry, a compound with nearly ideal $\left(\frac{c}{a}\right)$ or positive $\Delta\left(\frac{c}{a}\right)$ ratio therefore prefers to stabilize in ZB symmetry, satisfying the isotropic distribution completely.

6. Summery

Using NMTO-downfolding technique we have revisited the problem of ZB vs WZ symmetry in case of $A^N B^{8-N}$ semiconductors. In particular, we have considered the CdX series with X =S, Se, Te. Our computed ionicity factors using accurate NMTO-downfolding successfully brings out the right trend within the CdX series - CdS being most ionic stabilizes in WZ symmetry while CdSe and CdTe being more covalent stabilizes in ZB symmetry. Our NMTO constructed Wannier functions corresponding to only valence bands provide nice demonstration of this fact. The tendency towards ZB stability is governed by the covalency which prefers isotropic nature of the tetrahedral bonds.

7. Acknowledgment

S.D thanks CSIR for financial support and TSD acknowledges DST for support through Swarnajayanti fellowship.

References

- [1] W. A. Harrison, *Electronic Structure and the Properties of Solids* (Freeman, San Francisco, 1980).
- [2] J. C. Phillips, *Bonds and Bands in Semiconductors* (Academic, New York, 1973)
- [3] G. A. Jeffrey, G. S. Parry and R. L. Mozzi, *J. Chem. Phys.* **25**, 1024(1956)
- [4] F. Keffer and A. M. Portis, *J. Chem. Phys.* **27**, 675(1957)
- [5] J. C. Phillips and Van Vechten, *Phys. Rev. Lett.* **22**, 705(1969)
- [6] J. C. Phillips, *Rev. Mod. Phys.* **42**, 317(1970); J. A. Van Vechten, *Phys. Rev.* **187**, 1007(1969)
- [7] P. Lawaetz, *Phys. Rev. B* **5**, 4039(1972)
- [8] J. S. John and A. N. Bloch, *Phys. Rev. Lett.* **33**, 1095(1974)
- [9] A. Zunger and M. L. Cohen, *Phys. Rev. Lett.* **41**, 53(1978)
- [10] A. Zunger, *Phys. Rev. Lett.* **44**, 582(1980); A. Zunger, *Phys. Rev. B* **22**, 5839(1980)
- [11] N. E. Christensen, S. Satpathy and Z. Pawlowska, *Phys. Rev. B* **36**, 1032(1987)
- [12] C.-Y. Yeh, Z. W. Lu, S. Froyen and A. Zunger, *Phys. Rev. B* **45**, 12130(1992); C.-Y. Yeh, Z. W. Lu, S. Froyen and A. Zunger, *Phys. Rev. B* **46**, 10086(1992)
- [13] E. S. Rittner and J. H. Schulman, *J. Phys. Chem.* **47**, 537(1943)
- [14] V. A. Fedorov, V. A. Ganshin and Yu. N. Korkishko, *Phys. Stat. Sol.* **126**, K5(1991)
- [15] M. Kh. Rabadanov, I. A. Verin, Yu. M. Ivanov and V. I. Simonov, *Kristallografiya* **46**, 703(2001)
- [16] S. A. Semiletov, *Trudy Instituta Kristallografii, Akademiya Nauk SSSR*(1955), 1955(11), 121 - 123(from ICSD)
- [17] O.K. Andersen and T. Saha-Dasgupta, *Phys. Rev. B* **62**, R16219 (2000) and references there in.
- [18] P. D. Lao, Y. Guo, G. G. Siu and S. C. Shen, *Phys. Rev. B* **48**, 11701 (1993).
- [19] A. W. Stevenson and Z. Barnea, *Acta Cryst.* **B40**, 530(1984)
- [20] D. Vanderbilt, *Phys. Rev. B* **41**, 7892 (1990).
- [21] G. Kresse and J. Hafner, *Phys. Rev. B* **47**, RC558 (1993); *Phys. Rev. B* **48**, 13115 (1993); *Phys. Rev. B* **49**, 14251 (1994).
- [22] O. Zakharov, A. Rubio, X. Blase, M. L. Cohen and S. G. Louie, *Phys. Rev. B* **50**, 10780 (1994).
- [23] N. Marzari and D. Vanderbilt, *Phys. Rev. B* **56**, 12847(1997).

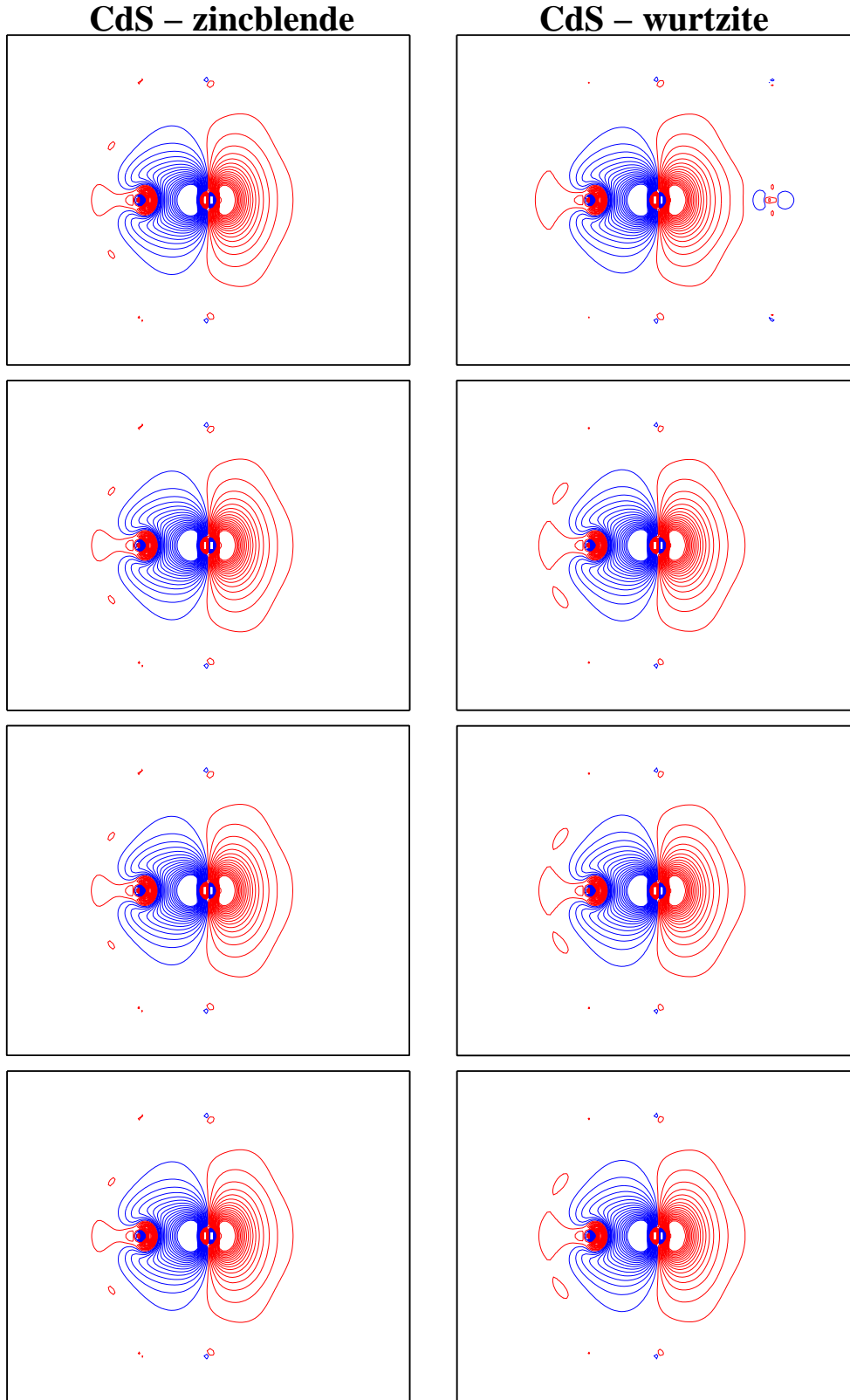


Figure 4. The contour plots show the p-MTO of S along the four nearest neighbor tetrahedral directions in ZB structure (left panels; from top to bottom they are $p[111]$, $p[\bar{1}\bar{1}\bar{1}]$, $p[\bar{1}1\bar{1}]$, $p[\bar{1}\bar{1}1]$) and in WZ structure (right panels; from top to bottom they are $p[001]$, $p[1, 0, \frac{u}{\sqrt{3}}\frac{c}{a}]$, $p[\frac{1}{2}, -\frac{\sqrt{3}}{2}, -\frac{2}{\sqrt{3}}u\frac{c}{a}]$, $p[\frac{1}{2}, \frac{\sqrt{3}}{2}, -\frac{2}{\sqrt{3}}u\frac{c}{a}]$) of CdS. The contours chosen are same as in Fig. 3

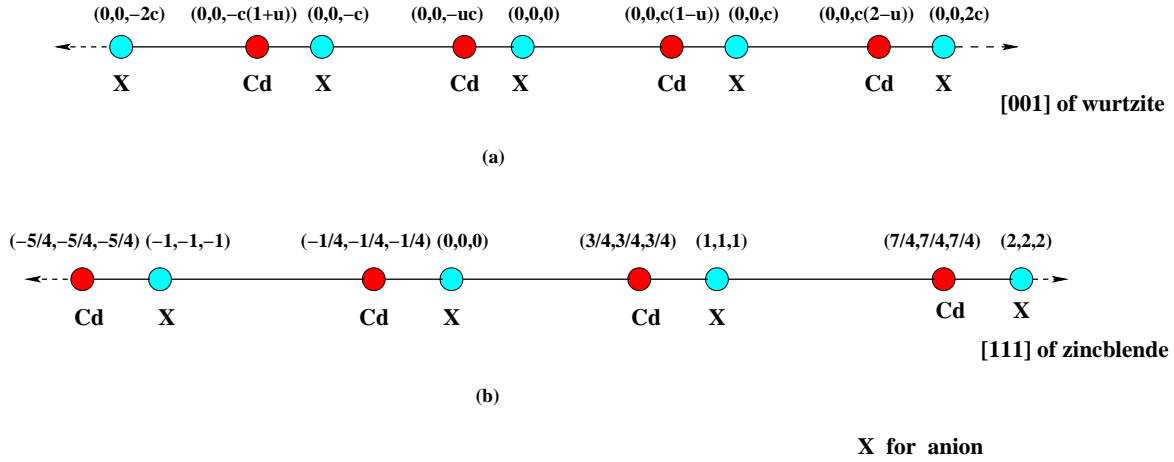


Figure 5. (a) Positions of atoms along [001] direction of wurtzite structure, (b) positions of atoms in unit of lattice constant along [111] direction of zincblende structure.

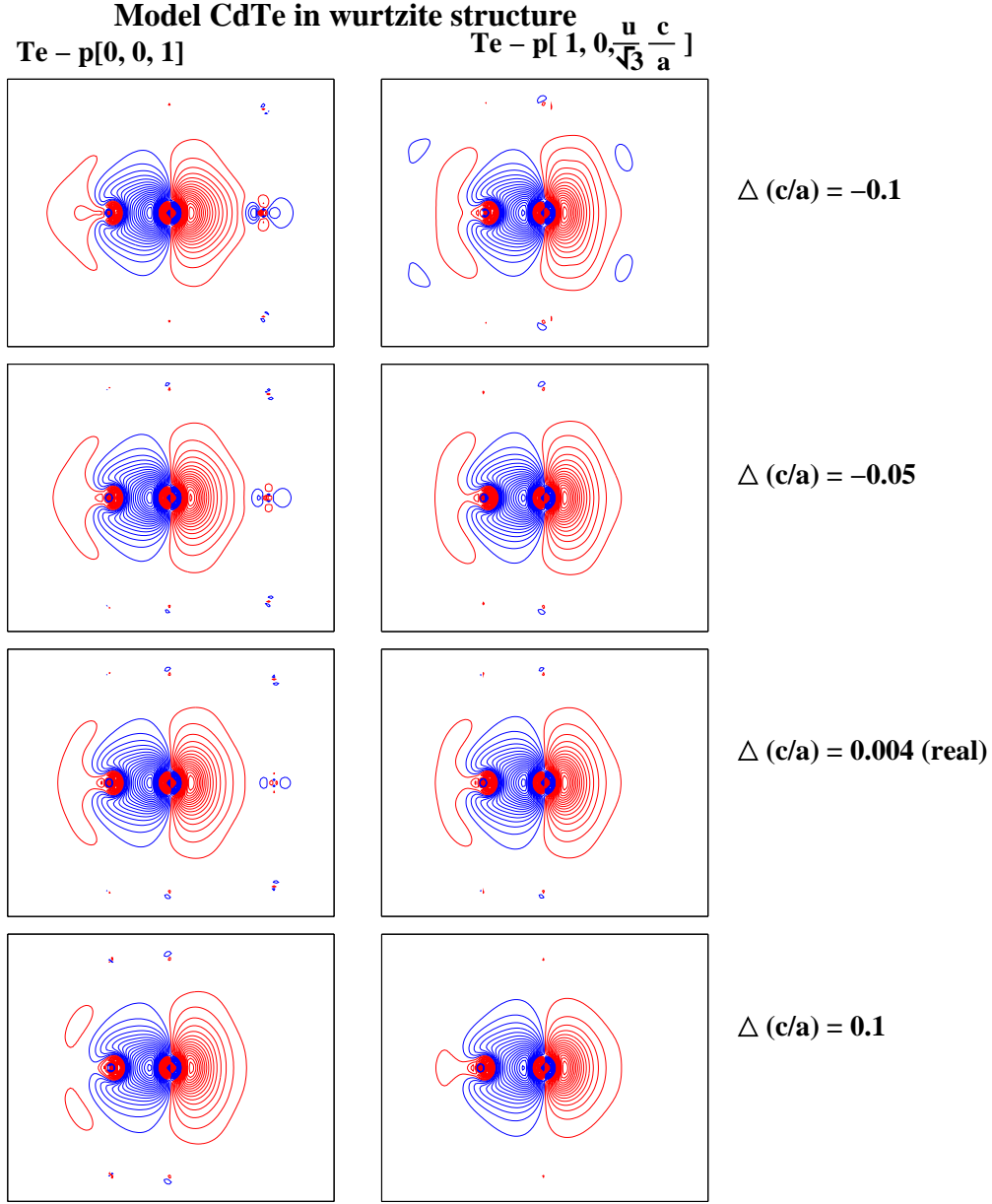


Figure 6. The above contour plots show the p-MTO of Te in WZ structure of model CdTe. The top panels correspond to p[001] and bottom panels correspond to p[1, 0, $\frac{u}{\sqrt{3}} \frac{c}{a}$]. From left to right ionicity decreases and covalency increases and distribution becomes more isotropic. The contours chosen are same as in Fig.3